Energy Transfer in Charge Exchange Collisions between Slow Ions and Rydberg Atoms

D. S. Fisher, C. W. Fehrenbach, and S. R. Lundeen
Department of Physics, Colorado State University, Fort Collins, Colorado 80523

E. A. Hessels
Department of Physics, York University, Toronto, Ontario, Canada M3J 1P3

B. D. DePaola
Department of Physics, Kansas State University, Manhattan, Kansas 66506
(Received 26 January 1998)

Charge transfer collisions between slow ions and Rydberg atoms have been studied for ion charges $q = 1-4$, using resonant laser excitation to detect specific energy states of the collision products. The data collected show a clear resonance in the capture cross section to a particular energy state as the binding energy of the Rydberg target is varied. The resonance position differs significantly from the predictions of the classical overbarrier model, and its width becomes very small (0.025 eV) at the lowest velocities studied. [S0031-9007(98)06812-4]

PACS numbers: 34.70.+e, 34.60.+z

Electron capture by slow ions from a Rydberg atom is a quasiresonant process in which the most probable binding energy of the captured electron is comparable to its original binding energy in the Rydberg atom target [1]. These collisions can be described in a simple manner classically as a three-body problem, but the quantum mechanical calculation quickly becomes intractable because of the large number of accessible states. While some classical models have been used to describe these collisions, notably the classical trajectory Monte Carlo model (CTMC) [2], the limitations of a classical description are not yet clear. Only a limited number of experimental studies have been reported, and these have studied the final state energy distributions indirectly by means of Stark ionization [1,3,4].

We report here a direct study of energy transfer in ion-Rydberg atom charge transfer collisions, using laser methods for both the preparation of the initial Rydberg state and the analysis of the final product state. The final state analysis uses a Doppler-tuned CO_2 laser to selectively excite a particular final state to a much higher level that is subsequently Stark ionized. We refer to this method of selective detection as resonant excitation Stark ionization spectroscopy, or RESIS. Since the range of final states that can be detected with this method is limited, we choose to measure the partial cross section for capture into a product state with fixed energy E_p over a broad range of target energies E_t. These measurements show the energy resonance in the entrance channel, as distinct from previous Stark ionization studies that displayed the resonance in the exit channel. Both methods probe the resonant behavior of the charge transfer collision, but our technique has the advantage of unambiguous identification of both the initial and final state energies. Although some of the methods of this study are similar to those we used in a previous experiment studying collisions of singly charged ions [5], this is the first reported use of the RESIS technique for detecting charged Rydberg states.

Experimental technique.—An ion beam of charge $q = 2-4$ (C^{2+}, C^{3+}, C^{4+}, Ar^{3+}, and Xe^{3+}) at velocities 0.031, 0.057, and 0.100 a.u. [6] is produced by the CRYEBIS ion source at Kansas State University [7]. Some ions capture an electron from a Rydberg target [8]. The Rydberg target is a dense beam of Rb vapor that undergoes three step cw laser excitation to the n_tF level, where $7 \leq n_t \leq 18$. While only the n_tF level is directly populated, a mirrorless maser action within the target puts about half of the population in the nearly degenerate $(n_t + 1)D$ state [8]. After the target, the beam passes through a double einzel lens that nearly eliminates the primary ion beam while maximizing the transmission of the charge capture beam of charge $q - 1$. The electric field in the einzel lenses does not exceed the field that would cause mixing between different n-levels near the measured level. The final state of interest is resonantly excited by a Doppler-tuned CO_2 laser to a highly excited state, which is then Stark ionized and energy tagged. An electrostatic analyzer is used to separate the Stark-ionized ions from the other ions and deflect them onto a Channeltron electron multiplier. A second measured quantity is the total charge capture beam, which is measured by retuning the electrostatic analyzer to collect the $q - 1$ ions formed in the Rydberg target.

A typical scan of the $n_p = 19$ to $n' = 51$ laser signal used for the measurements with $q = 2$ ions is shown in Fig. 1. The large peak contains unresolved contributions from $n_p = 19$, $L = 11-18$ states, and is used as an indicator of the $n_p = 19$ population in C^+. Similar transitions are used to monitor the populations of $n_p = 29$ for $q = 3$ and $n_p = 37$ for $q = 4$ ions [6]. The ratio between one of these RESIS signal amplitudes and the total charge transfer beam is the primary measured quantity for this study.

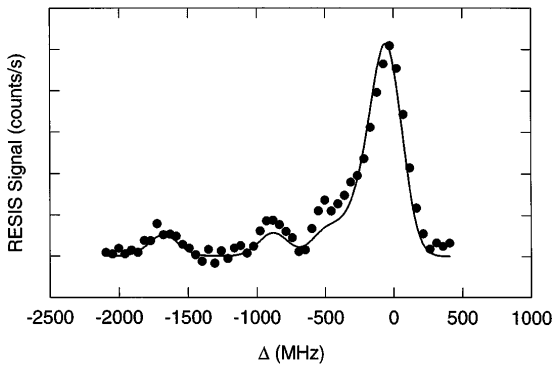

FIG. 1. RESIS excitation spectrum for $n_p = 19$ or $n' = 51$ in C^+. The large peak represents excitation of $n_p = 19$, $L = 11-18$. The two well resolved peaks to the left are $L = 8$ and $L = 9$. The horizontal axis is the difference of the hydrogenic transition frequency, 1047.120 cm^{-1}, and the Doppler-tuned CO_2 laser frequency. The solid line is a theoretical spectrum assuming a C^{2+} dipole polarizability of $3.56a_0^3$ and a Gaussian instrumental line shape with 250 MHz width.

This ratio, which we refer to as R_p, is proportional to the fraction of the total charge transfer product formed in the selected state. It is relatively easy to measure precisely, because it is independent of the Rydberg target thickness. As the binding energy of the Rydberg target is varied R_p changes, reflecting the changes in the final state population distribution. In this study we measured the variation of R_p over a range of targets $7 \leq n_t \leq 18$ for several choices of ion charge and velocity. The ions studied were of charge $q = 2$, 3, 4 at $v = 0.1$ a.u., and charge $q = 3$ at $v = 0.057$ and 0.031 a.u.

The experimentally measured ratio, R_p, is proportional to σ_p/σ_T, where σ_p is the partial cross section for charge transfer to a particular n_p and range of l states [6], and σ_T is the total charge transfer cross section. Although in principle, both factors, σ_p and σ_T, could be evaluated from theory and the ratio checked directly, σ_p contains the most interesting physics. In order to simplify the interpretation of our data, we choose to multiply the measured values of R_p by a theoretical value of σ_T, thus obtaining an estimate of σ_p alone. Since the dependence of σ_T on both q and v has been checked in a separate experiment [9], this does not require an unreasonable reliance on theory. The product of our measured fraction, R_p, and this estimate of σ_T [10] gives σ_p for each n_t up to an unknown constant. The results are plotted in Fig. 2 for the five ions of this study and the $q = 1$, $v = 0.1$ a.u. ion studied previously [5].

Since the CO_2 laser probes the population of the n_p level 45 cm downstream of the Rydberg target, spontaneous and black-body stimulated radiative decay and cascades alter the populations somewhat. We have simulated and corrected for these effects using predicted population distributions in all excited states obtained from CTMC. Generally only a small correction of the data is needed to infer the original population at the Rydberg target, since the radiative lifetimes of the n_p levels are long, 5–20 μs,

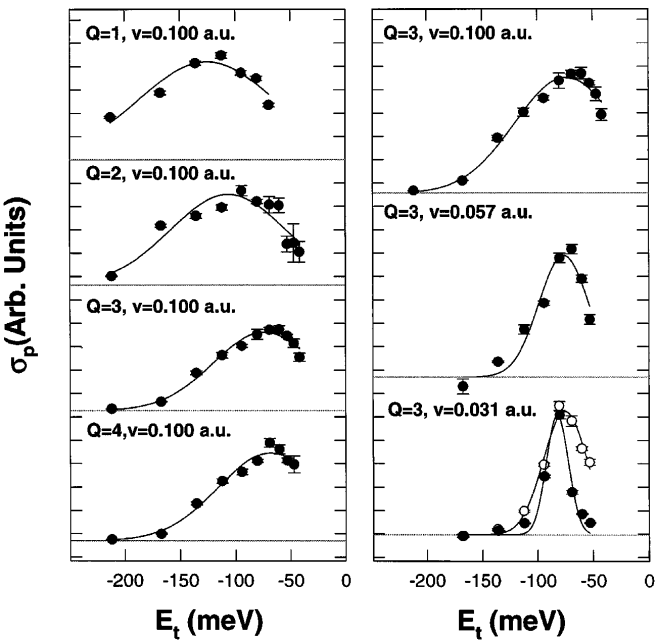

FIG. 2. Partial cross sections for formation of a final state of fixed energy E_p as a function of the energy of the Rydberg target for all six choices of ion charge and velocity. E_p is approximately -150 meV in all cases [6]. Where open points are shown, they represent the results prior to cascade corrections. The solid lines are fits to the Gaussian parametrization of Eq. (1).

compared with the transit time of 2–6 μs. However, in the case of the slowest projectiles, the cascade correction is quite significant when the directly populated states lie above the state detected. One ambiguity in these calculations is the possible redistribution of the population within the various L states of common n by electric fields in the double einzel lens. The degree of redistribution depends on the detailed conditions of entry and exit from the fields. As a test of the significance of such mixing, we simulated the cascade corrections with both a complete L mixing and no L mixing at the double einzel lens. We corrected the data with the average of these two simulations; the difference between them was insignificant.

Figure 2 shows the final results for σ_p, after corrections for cascades, plotted versus the energy of the Rydberg target. Remarkably, when plotted in this way all the results appear to be simple symmetric curves. The smooth curves in Fig. 2 are fits to a Gaussian parametrization:

$$\sigma_p(E_t, E_p) = A \exp\left[-2.77\left(\frac{E_t - \kappa E_p}{W}\right)^2\right], \quad (1)$$

where E_p is the fixed binding energy of the detected state, E_t is the binding energy of the target, and A, κ, and W are fitting parameters. The parameters κ and W, which represent, respectively, the position and full width at half maximum of these symmetric curves, are shown in Table I for all six ions of this study. Also shown for comparison are the values of κ and W obtained from similar fits of CTMC calculations of σ_p.

TABLE I. Gaussian parameters resulting from fits of partial cross section distributions to Eq. (1). Columns 2 and 3 show parameters for experimental data, and columns 4 and 5 show the parameters for the CTMC simulations.

	Experiment		CTMC	
$(q, v$(a.u.))	κ	W(eV)	κ	W(eV)
(1, 0.100)	0.92(4)	0.149(17)	1.02(3)	0.183(18)
(2, 0.100)	0.69(3)	0.120(13)	0.757(13)	0.134(5)
(3, 0.100)	0.508(14)	0.103(7)	0.599(6)	0.108(3)
(4, 0.100)	0.43(3)	0.110(10)	0.518(4)	0.093(2)
(3, 0.057)	0.522(14)	0.057(7)	0.510(9)	0.045(3)
(3, 0.031)	0.566(8)	0.025(2)	0.569(3)	0.020(1)

The measured values of κ and W lead to some general conclusions about the internal energy transfer in ion-Rydberg charge transfer. First, the fact that κ is not equal to one for $q > 1$ shows that the most probable binding energy of the charge transfer product is not equal to that of the target, but rather increases with q for constant target energy. This is a widely anticipated result and appears at least roughly consistent with the predictions of CTMC [2]. Second, the decrease of W with q indicates that the range of target energies that can yield a particular E_p decreases with q, but somewhat more slowly than κ. Comparison of the results obtained for $q = 3$ ions at three velocities shows only a small change of κ with v, implying the most probable E_p for fixed E_t is at most a weak function of v. In contrast, the width parameter W varies dramatically with velocity. Within the precision of this study, it appears to be *linear* in velocity, demonstrating that the charge transfer process becomes extremely energy selective at sufficiently low velocities. For the slowest ion studied here, $W = 0.025$ eV.

A closer look at the variation of κ with q is provided by Fig. 3, which plots $(1 - \kappa)$ vs q. Also shown in Fig. 3 are two widely cited classical predictions. The classical overbarrier model (COB) predicts [11]

$$\kappa^{\mathrm{COB}} = \frac{1 + 2\sqrt{q}}{q + 2\sqrt{q}}. \tag{2}$$

This leads to one of the solid curves shown in Fig. 3. It is clearly different from the measurements. Another classical prediction is an empirical estimate obtained by examination of CTMC results for several values of q [12],

$$\kappa^{\mathrm{CTMC}} \cong \frac{1}{\sqrt{q}}. \tag{3}$$

This leads to the other solid curve in Fig. 3, which is also inconsistent with our measurements. It is reasonably consistent with the κ's obtained by fitting the CTMC simulations for this experiment, taken from Table I and also shown in Fig. 3.

The deviation of κ^{COB} from the measurements may have a simple explanation. The COB model is closely analogous to the simplest model of Stark ionization of atoms, which predicts an ionizing field of $E_{cl} = 1/16n^4$ a.u. While this may be correct for atomic ground states, it is known to underestimate the diabatic ionization fields of Rydberg states by a factor of 1.8 to 3.6, depending on the Stark state [13]. Therefore, we might expect the COB model to underestimate the field required to "ionize" the Rydberg target and cause charge capture by a similar factor. This would imply an overestimate of the capture radius by the square root of that factor, or about 1.6. The capture radius is expected to be closely related to the binding energy of the products. This is a consequence of conservation of total energy in the collision. For $q > 1$, the collision products are both charged and gain kinetic energy as they repel each other after charge transfer. To conserve total energy, the product state is more tightly bound than the target state by the amount of kinetic energy gained,

$$\Delta E \equiv E_p - E_t \approx \frac{(q - 1)e^2}{r_c}, \tag{4}$$

where r_c is the radius where capture occurs. The COB model gives exactly the same equation [14]. For constant E_p, the quantity $(1 - \kappa)$ plotted in Fig. 3 is proportional to $E_p - E_t$; thus, if the COB model does overestimate the capture radius by a factor of 1.6 this leads to an underestimate of $(1 - \kappa)$ by a similar factor. Indeed, a correction factor of 1.56(4) gives very good agreement with the measured κ's, as is shown by the dashed line in Fig. 3. This suggests that the COB model could be considerably improved by incorporating a more realistic description of the "ionization" of the Rydberg electron.

The deviation of κ^{CTMC} from the measurements, although smaller, is still significant. It is much more difficult to understand since CTMC presumably models the

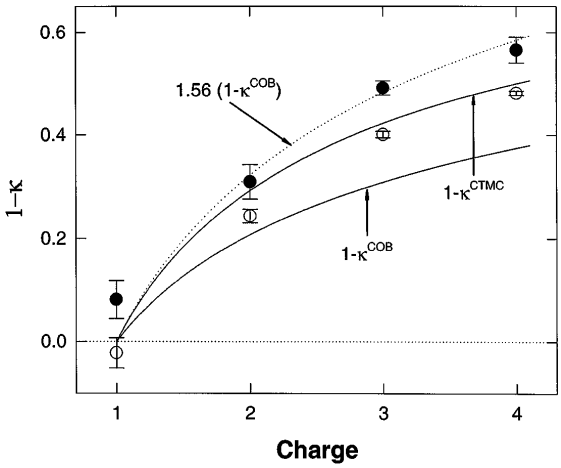

FIG. 3. Measured values of κ for ions of velocity 0.1 a.u., from Table I, are shown as solid points and plotted as a function of ion charge. They are compared with two predictions from classical models, κ^{COB} and κ^{CTMC}. Neither prediction agrees with the measurements. The open points show the results of Gaussian fits of CTMC simulations, and are approximately consistent with κ^{CTMC}. A simple modification of κ^{COB}, discussed in the text and shown here as a dashed line, gives good agreement with the data.

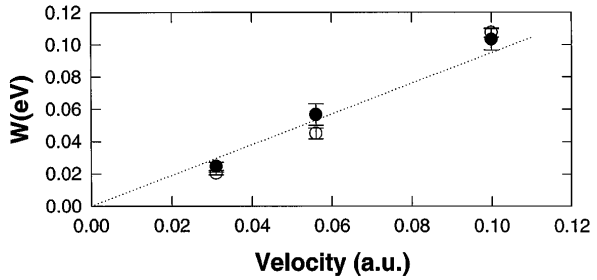

FIG. 4. Measured values of W, the resonance full width at half maximum, plotted versus the ion velocity for ions of charge $q = 3$. The solid points are measurements and the open points are fits of CTMC simulations, both from Table I. The dashed line is a linear fit of the measurements, which has the form predicted by an uncertainty principle argument.

Rydberg ionization more realistically. The one obvious limitation of CTMC, the neglect of tunneling, is probably not responsible for the deviation, since it would produce a deviation of the opposite sign. Finally, we note that previous studies of charge capture by $q = 8$ ions using Stark ionization [3,4] are not precise enough to discriminate between the three curves in Fig. 3.

The variation of W with v is illustrated in Fig. 4. For comparison, a linear fit through zero is shown as a dashed line. From one point of view, this dependence on v may seem unremarkable. Since it is known that σ_T is approximately constant at low velocities [8], one might characterize the collisions as taking place over a time interval $\Delta t \approx \sqrt{\sigma_T}/v$. Then, based on the energy-time uncertainty principle, the width W would be given by

$$W = A\frac{h}{\Delta t} = Ah\frac{v}{\sqrt{\sigma_T}}, \tag{5}$$

where h is Planck's constant, v is the ion's velocity, and A is a dimensionless constant of order one. The dashed line in Fig. 4 is Eq. (5) with $A = 6.3$ [15]. Although no quantum mechanical theory of this process yet exists, one would expect a width of this form to result from such a calculation. On the other hand, CTMC, a purely classical calculation, predicts widths in agreement with our measurements, as shown by the open points in Fig. 4 taken from Table I. Therefore, there may be an alternative explanation for the dependence on v.

In summary, this study has determined the general characteristics of internal energy transfer in slow ion-Rydberg collisions, with $q = 1$–4. The energy transfer is found to be highly selective at the lowest velocities studied, and to have a width consistent with a simple uncertainty principle argument. The resonance position differs significantly from the classical overbarrier prediction, possibly because that model underestimates the field necessary to "ionize" the Rydberg target. The predictions of CTMC are in general agreement with our measurements, except for small deviations in the resonance position.

This work was supported by the Division of Chemical Sciences, Office of Basic Energy Sciences, Office of Basic Energy Research, and the U.S. Department of Energy.

[1] K. B. MacAdam, L. G. Gray, and R. G. Rolfes, Phys. Rev. A **42**, 5269 (1990).
[2] J. Pascale, R. E. Olson, and C. O. Reinhold, Phys. Rev. A **42**, 5305 (1990).
[3] A. Pesnelle *et al.*, Phys. Rev. A **54**, 4051 (1996).
[4] A. Pesnelle *et al.*, Phys. Rev. Lett. **74**, 4169 (1995).
[5] D. S. Fisher *et al.*, Phys. Rev. A **56**, 4656 (1997).
[6] The specific ions and RESIS transitions used were as follows: $v = 0.100$: $^4He^+$, $n_p = 10$ ($L = 7$–9) to $n' = 30$; $v = 0.100$: $^{13}C^{2+}$, $n_p = 19$ ($L = 11$–18) to $n' = 51$; $v = 0.100$: $^{13}C^{3+}$, $n_p = 29$ ($L = 13$–28) to $n' = 71$; $v = 0.100$: $^{13}C^{4+}$, $n_p = 37$ ($L = 0$–36) to $n' = 85$; $v = 0.057$: $^{40}Ar^{3+}$, $n_p = 29$ ($L = 13$–28) to $n' = 71$; $v = 0.031$: $^{136}Xe^{3+}$, $n_p = 29$ ($L = 16$–28) to $n' = 71$.
[7] M. P. Stöckli *et al.*, Phys. Scr. **T71**, 188 (1997).
[8] C. W. Fehrenbach, S. R. Lundeen, and O. L. Weaver, Phys. Rev. A **51**, R910 (1995).
[9] M. T. Huang *et al.*, J. Phys. B **30**, 2425 (1997).
[10] The total cross sections calculated by CTMC for the ions and targets used are as follows in units of 10^{-12} cm^2, He^+ $n_t = 7$–14 [0.68, 1.15, 1.77, 2.31, 2.56, 2.48, 2.40, 2.27]; C^{2+} $n_t = 8$–18 [3.17, 4.99, 7.17, 9.37, 11.4, 12.12, 12.51, 12.24, 11.66, 11.32, 10.74]; C^{3+} $n_t = 8$–18 [5.31, 8.45, 12.46, 16.93, 21.63, 25.5, 28.0, 29.1, 29.3, 29.3, 27.7]; C^{4+} $n_t = 8$–17 [7.49, 11.98, 17.49, 24.59, 32.6, 40.1, 46.9, 50.1, 53.3, 53.3]; Ar^{3+} $n_t = 9$–16 [8.42, 12.93, 17.68, 24.81, 36.1, 50.1, 66.3, 84.9]; Xe^{3+} $n_t = 9$–16 [9.09, 14.06, 21.16, 30.0, 41.0, 53.5, 68.1, 84.5].
[11] H. Ryufuku, K. Sasaki, and T. Watanabe, Phys. Rev. A **21**, 745 (1980).
[12] A. P. Hickman, R. E. Olson, and J. Pascale, in *Rydberg States of Atoms and Molecules*, edited by R. F. Stebbings and F. B. Dunning (Cambridge University Press, Cambridge, England, 1983), Eq. (80).
[13] T. F. Gallagher, *Rydberg Atoms* (Cambridge University Press, Cambridge, England, 1994).
[14] Equation (2.3) in [11] generalized for arbitrary target state is $-1/2n_t^2 - q/r_c = -q^2/2n_p^2 - 1/r_c$ from which Eq. (4) follows.
[15] For the linear fit, σ_T is taken to be 34×10^{-12} cm^2, the average σ_T for $n_t = 13$, the peak of σ_p, for the three velocities [9]. Including the small variations of σ_T gives an even better fit of the observed widths.